GEOPHYSICAL RESEARCH LETTERS, VOL. 35, L11506, doi:10.1029/2008GL033985, 2008

Accelerated Arctic land warming and permafrost degradation during rapid sea ice loss

David M. Lawrence,[1] Andrew G. Slater,[2] Robert A. Tomas,[1] Marika M. Holland,[1] and Clara Deser[1]

Received 13 March 2008; revised 14 April 2008; accepted 24 April 2008; published 13 June 2008.

[1] Coupled climate models and recent observational evidence suggest that Arctic sea ice may undergo abrupt periods of loss during the next fifty years. Here, we evaluate how rapid sea ice loss affects terrestrial Arctic climate and ground thermal state in the Community Climate System Model. We find that simulated western Arctic land warming trends during rapid sea ice loss are 3.5 times greater than secular 21st century climate-change trends. The accelerated warming signal penetrates up to 1500 km inland and is apparent throughout most of the year, peaking in autumn. Idealized experiments using the Community Land Model, with improved permafrost dynamics, indicate that an accelerated warming period substantially increases ground heat accumulation. Enhanced heat accumulation leads to rapid degradation of warm permafrost and may increase the vulnerability of colder permafrost to degradation under continued warming. Taken together, these results imply a link between rapid sea ice loss and permafrost health.
Citation: Lawrence, D. M., A. G. Slater, R. A. Tomas, M. M. Holland, and C. Deser (2008), Accelerated Arctic land warming and permafrost degradation during rapid sea ice loss, *Geophys. Res. Lett.*, *35*, L11506, doi:10.1029/2008GL033985.

1. Introduction

[2] Over the past several decades, Arctic sea ice extent has been steadily shrinking. Due to the ice-albedo feedback, this reduction in ice cover has contributed to an observed amplification of Arctic warming [*Serreze and Francis*, 2006]. In general, Arctic sea ice area is a robust inverse predictor of Arctic land air temperature (T_{air}). Over the period 1979 to 2006, June to September detrended sea ice area (data from *Stroeve and Meier* [1999, updated 2006]) and detrended western Arctic land air temperature (65°–80°N, 90°–270°E; data from Climate Research Unit, CRUTEM3 [*Jones et al.*, 2006]) are correlated at −0.59 ($P < 0.01$).

[3] In September 2007, the annual minimum sea ice extent shattered the previous observational-record low [*Stroeve et al.*, 2008]. Preliminary CRUTEM3 data indicate that 2007 August to October western Arctic land temperatures were the warmest of the last 30 years (+2.3°C warmer than the 1978 to 2006 average). The striking sea ice decline in 2007 raises the specter that a period of abrupt sea ice loss, such as those simulated in Community Climate System Model (CCSM3) 21st century A1B simulations [*Holland et al.*, 2006b], is a distinct possibility. Rapid sea ice loss events (RILEs) in CCSM3 typically last between 5 and 10 years and exhibit negative sea ice extent trends that are roughly 4 times larger than average simulated (or recently observed) trends. Analogous abrupt sea ice loss events are found in roughly 50% of the Intergovernmental Panel on Climate Change Fourth Assessment Report (IPCC AR4) coupled models. CCSM3 exhibits both a reasonable simulation of present-day sea ice conditions (extent and thickness) and replicates the rate of sea ice loss over the last few decades [*Holland et al.*, 2006a].

[4] Whether or not the 2007 sea ice record minimum is a precursor of a sustained period of rapid loss remains to be seen, but it provides motivation to assess the potential consequences for adjacent land climate. Here, we evaluate Arctic land temperature response to RILEs in CCSM3. We find that the secular 21st century land warming trend is augmented by a factor of 3.5 during RILEs, which is likely to have adverse impacts on permafrost. Through idealized experiments with the Community Land Model (CLM), we assess the impact of a RILE and its timing on permafrost.

2. Arctic Land Temperature Trends During Rapid Sea Ice Loss Events

[5] Nine RILEs are identified [*Holland et al.*, 2006b] across the eight member CCSM3 A1B 21st century ensemble [*Meehl et al.*, 2006] (an overview of CCSM3 and an assessment of its sea ice simulation is provided by *Collins et al.* [2006a] and *Holland et al.* [2006a], respectively). By computing a lagged composite of sea ice extent anomalies across the nine events, we form a picture of the typical sea ice extent trajectory during abrupt loss periods (Figure 1a). A corresponding composite for western Arctic October to December (OND) land T_{air} reveals an increased warming rate during RILEs (Figure 1a). Figure 1b shows the western Arctic linear T_{air} trend during and outside RILEs. Warming is accelerated during RILEs throughout most of the year with statistically significant increases in warming rates apparent in the summer and early autumn, likely due to increased open water area, as well as in late autumn and winter, when the thinner ice pack less efficiently insulates the atmosphere from the comparatively warm ocean water below. Accelerated warming spans most of the terrestrial western Arctic juxtaposed to the area of sea ice contraction in CCSM3. It is strongest along the Arctic coast where it is as high as 5°C decade^{-1} in the autumn, but a signal of enhanced warming can extend 1500 km inland (Figure 1c). Annually averaged, the warming trend during RILEs is

[1]Climate and Global Dynamics Division, National Center for Atmospheric Research, Boulder, Colorado, USA.
[2]Cooperative Institute for Research in Environmental Sciences, University of Colorado, Boulder, Colorado, USA.

0094-8276/08/2008GL033985$05.00

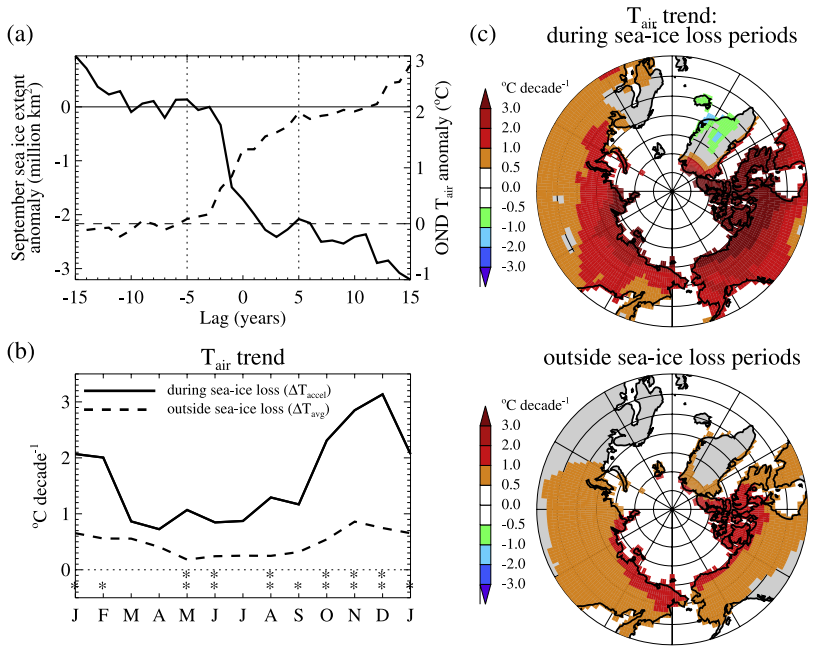

Figure 1. (a) Composite anomaly time series of September sea ice extent (solid line) and OND T_{air} (dashed line) over Arctic land area (65°–80°N, 60°–300°E). Composites are formed by averaging nine 31-yr anomaly time series. Each of the nine time series are centered about the mid-point of a CCSM3 rapid sea ice loss event (lag 0 years) and are anomalies from the lag −10 to −5 year mean. (b) Average monthly Arctic land air temperature trends during rapid sea ice loss periods and outside sea ice loss periods. The difference in trends are statistically significant at the 90% (single asterisk) and 95% (double asterisk) levels. (c) Maps of air temperature trends for OND during and outside abrupt sea ice loss periods.

3.5 times greater than outside these periods (1.60°C decade^{-1} versus 0.46°C decade^{-1}).

[6] Corresponding analyses are performed for precipitation (P), snow depth, specific humidity (q_{air}), and downwelling longwave (LW↓) and solar (SW↓) radiation. Specific humidity and LW↓ exhibit accelerated trends in harmony with accelerated T_{air} trends. Trends during RILEs for snow depth, P, and SW↓ are not statistically differentiable from the secular 21st century trends for these quantities.

[7] The acceleration in Arctic land warming during RILEs raises an obvious question as to whether or not accelerated warming is predominantly a response to or a forcing of rapid sea ice loss. *Holland et al.* [2006b] argue that abrupt sea ice transitions in CCSM are thermodynamically driven with thinning ice leading to enhanced open water production and more solar radiation absorbed. An abrupt ice loss event can then be triggered by an episodic increase in ocean heat transport to the Arctic. Rising T_{air} is not cited as a principal triggering mechanism.

[8] The intuitive interpretation that warming over land is a response to sea ice loss is supported by a set of atmosphere-land simulations that isolate the influence of future versus present-day sea ice conditions on climate (e.g., separate from greenhouse gas forcing). Two 60-yr simulations with the Community Atmosphere Model (CAM3 [*Collins et al.*, 2006b]) coupled to CLM3 were conducted. The first simulation is forced with 1980–1999 monthly average sea ice thickness and distribution from CCSM3. The second simulation uses the thinner and contracted 2080–2099 sea-ice conditions from CCSM3 A1B integrations. Both simulations use the same observed climatological sea surface temperatures. Differences in T_{air} due to sea ice loss show a pattern of warming (Figure 2) that is consistent with the accelerated warming pattern during rapid sea ice retreat in CCSM3 (Figure 1c). The annual cycle phase of the warming is also similar with the strongest warming occurring in autumn and early winter. Taken together, Figures 1 and 2 demonstrate that extensive and rapid sea ice loss results in strong and spatially extensive warming of Arctic land.

3. Impact of Accelerated Warming on Permafrost

3.1. Community Land Model

[9] CLM3.5 [*Oleson et al.*, 2008] is a process-based model of the land-surface that serves as the land component of the CCSM3. It calculates heat and radiation fluxes at the land-atmosphere interface, as well as temperature, humidity, and soil thermal and hydrologic states – including explicit treatment of soil freeze/thaw processes. Improvements over CLM3.5 include explicit representation of the thermal and hydrologic properties of organic soil [*Lawrence and Slater*, 2007] and an extension of the soil column to 50 m to represent the thermal inertia of deep ground [*Lawrence et al.*, 2008]. The model reasonably simulates observed soil temperature-depth-annual cycle relationships for tested locations in Siberia and Alaska [*Nicolsky et al.*, 2007; *Lawrence et al.*, 2008]. Soil vertical resolution is increased fourfold using 60, instead of 15, layers.

3.2. Synthetic Arctic Climatic Trend Scenarios

[10] In the CCSM3 A1B ensemble, RILEs initiate at years ranging from 2012 to 2045, with one ensemble member not exhibiting an abrupt event. Here, we construct four synthetic T_{air} trend scenarios that reflect the range of possibilities for an abrupt event with 10-yr long accelerated

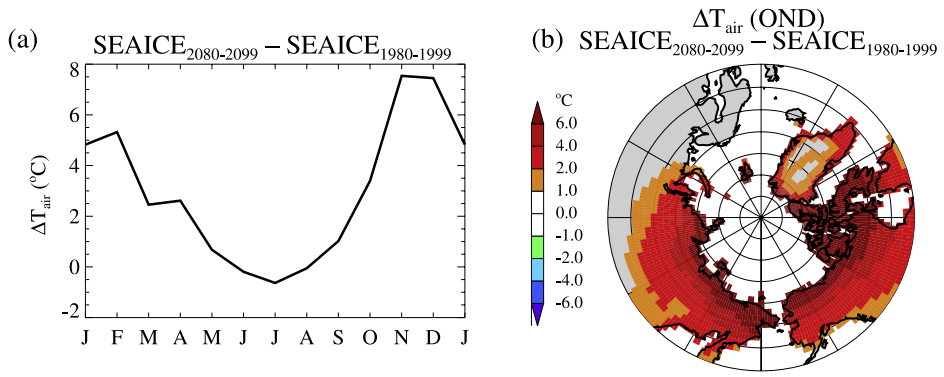

Figure 2. ΔT_{air} between simulations with prescribed 2080–2099 sea-ice conditions obtained from CCSM3 A1B 21st century ensemble and prescribed 1980–1999 sea-ice conditions obtained from CCSM3 20th century ensemble. (a) Monthly ΔT_{air} over western Arctic land (65°–80°N, 60°–300°E). (b) Map of ΔT_{air} for OND.

warming periods occurring early (yrs 6–15, EARLY), in the middle (yrs 21–30, MID), or in the latter part (yrs 36–45, LATE) of a 50-yr period, or not at all (LINEAR) (see Table 1 and Figure 3a). Monthly T_{air} anomaly time series are constructed based on the calculated CCSM3 trends during and outside RILEs (Figure 1b) by recursively adding the monthly trend (°C yr^{-1}) year after year in the following manner, for example for the EARLY scenario,

$$T_{air}(m,y) = T_{air}(m,y-1) + \Delta T_{avg}(m) \qquad y = 1,2,3,4,5$$

$$T_{air}(m,y) = T_{air}(m,y-1) + \Delta T_{accel}(m) \qquad y = 6,7,8,\ldots 15$$

$$T_{air}(m,y) = T_{air}(m,y-1) + \Delta T_{avg}(m) \qquad y = 16,17,18,\ldots 50$$

where m is the month (m = 1, 2, 3, . . . 12), y is the year, and ΔT_{avg} and ΔT_{accel} are the monthly T_{air} trends as in Figure 1b. For the LINEAR scenario,

$$T_{air}(m,y) = T_{air}(m,y-1) + \frac{4\Delta T_{avg}(m) + \Delta T_{accel}(m)}{5}$$
$$y = 1,2,3,\ldots 50.$$

The annual mean temperature change at year 50 is exactly the same for each scenario (+3.5°C).

[11] We also adjust q_{air} so that RH is conserved as T_{air} rises. Since LW↓ is a function of T_{air} and q_{air}, their modification influences LW↓ forcing. Hence, the accumulated LW↓ anomaly is highest in EARLY, while it is exactly the same in LINEAR and MID (Figure 3b)]. Due to the lack of statistically significant alterations in P or SW↓ trends during RILEs, we do not apply trends for these quantities. These experiments are idealized and are designed to focus on the impact of accelerated warming in the absence of other climate perturbations. CCSM3 and most other GCMs project that the high-latitudes will become wetter and cloudier during the 21st century [*IPCC*, 2007]. The actual rate of soil warming will be due to the combined changes in T_{air}, P, snow depth, and other forcings (e.g., vegetation, SW↓, disturbance, etc.).

[12] For each synthetic warming scenario, 50-yrs of gridded forcing data are created by adding T_{air}, q_{air}, and LW↓ anomalies to observed 3-hourly time series from an arbitrary year. Prior to integrating the model with the synthetic trend scenarios, CLM is spun-up for 400 years with repeat year 2000 forcing data [*Qian et al.*, 2006].

3.3. Results From Warming Scenario Experiments

[13] The impact of accelerated warming is shown for three illustrative ground conditions representing differing initial permafrost states (warm to cold) (Figures 3c and 3d). These cases exhibit minimal snow depth change (<10%) over the 50-yr simulation. For initially cold permafrost, the timing of accelerated warming has little influence on the rate of active layer deepening. All four scenarios simulate an ~0.35m deepening of the active layer (Table 1). However, the soil heat content (SHC) gained in EARLY (191 MJ m^{-2}) is 30% larger than in LATE (147 MJ m^{-2}). The additional heat gained in EARLY corresponds to +0.41°C more column warming, thereby increasing vulnerability to subsequent thaw. For reference, this SHC difference due to the timing of accelerated warming is almost two-thirds the 70MJ m^{-2} estimated global average land heat gain for the period 1950 to 2000 [*Beltrami et al.*, 2002]. The SHC increase is 8% higher (+13 MJ m^{-2}, +0.11°C) in MID relative to LINEAR even though accumulated LW↓ is the same in both.

[14] For warm permafrost, the timing of accelerated warming has a more dramatic influence. In all four scenarios, DPT increases slowly at first but accelerates rapidly once a layer of perpetually unfrozen ground forms above the permafrost table (talik) at ~0.2m depth. This occurs much sooner in EARLY with accelerated warming instigating talik formation by year 12. By year 50, the warm permafrost soil column in EARLY has absorbed 900 MJ m^{-2}, 68% more than LATE, and the DPT is 3.6 m deeper compared to only 1.9m deeper in LATE. Accelerated warming in the middle of the simulation results in more heat gain and leads to greater DPT deepening than when warming is linear, even though total LW↓ forcing is the same.

4. Discussion

[15] Why does talik formation coincide with a strong increase in SHC accumulation rates? Taliks form when the

Table 1. Change in DPT and SHC From Year 1 to Year 50 for Three Representative Initial Permafrost States Identified by Annual Mean T_{soil} at The Permafrost Table in Year 1, $\overline{T_{soil}(PT, y=1)}$[a]

	$\overline{T_{soil}(PT, y=1)}$ organic layer max snow depth	−0.3°C 30 cm 34 cm		−1.5°C 15 cm organic 65 cm max snow		−5.8°C 15 cm 45 cm	
Experiment	Description	△DPT, m	△SHC, MJ m^{-2}	△DPT, m	△SHC, MJ m^{-2}	△DPT, m	△SHC, MJ m^{-2}
LINEAR	Linear trend	2.7	706	0.94	281	0.35	167
EARLY	Accelerated warming yrs 6–15	3.6	899	1.19	347	0.35	191
MID	Accelerated warming yrs 21–30	3.1	767	1.11	321	0.35	180
LATE	Accelerated warming yrs 36–45	1.9	532	0.87	254	0.35	147

[a]Surface Organic Layer Thickness and Annual Maximum Snow Depth are Listed for Reference.

downwelling summer heating wave extends deeper than the corresponding winter cooling wave, thereby preventing the talik from refreezing in winter and permitting heat to accumulate at depth as soil ice melts (e.g., perpetually high SHC zone in Figure 4). Near isothermal soil layers at ~0°C beneath the talik also limit cooling from below. Once the soil reaches this state, heat accumulates at the maximum depth of the heating wave and permafrost degrades rapidly.

[16] Recent observational evidence suggests that permafrost may be vulnerable to rapid warming. *Jorgenson et al.*

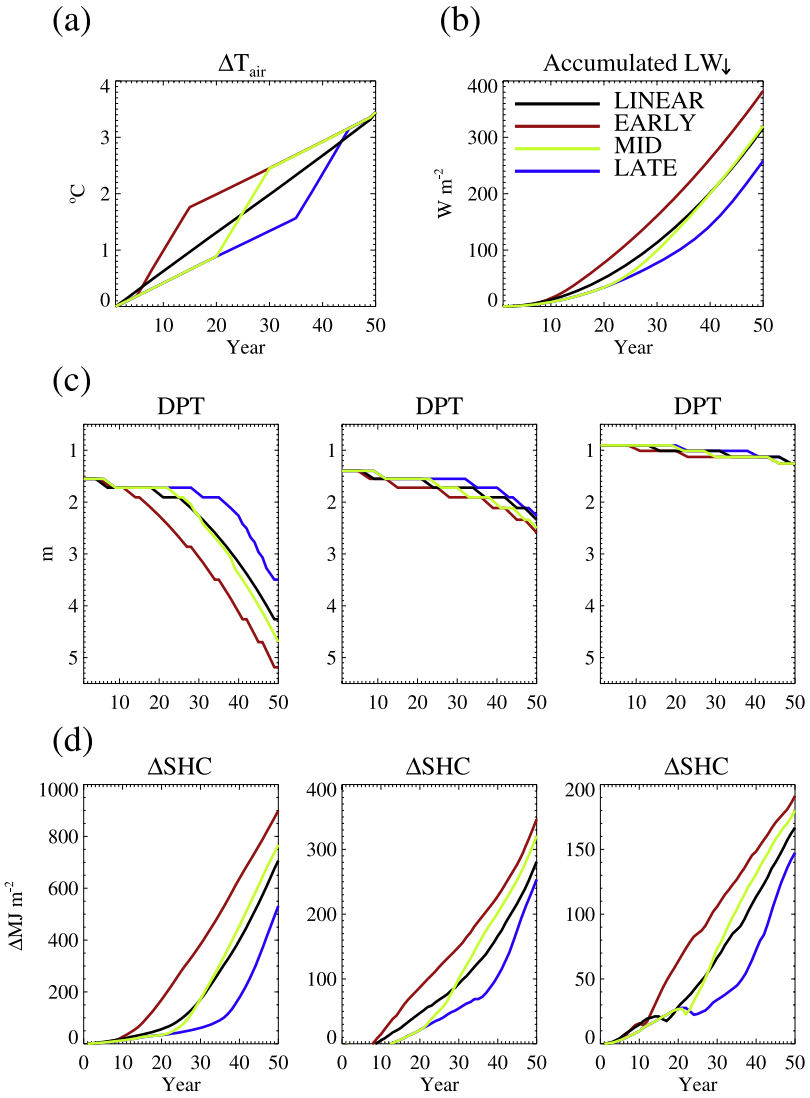

Figure 3. (a) Annual mean T_{air} anomaly time series for the four experiments. Note that monthly air temperature anomalies used in the forced experiments contain the annual cycle structure shown in Figure 1c. (b) Accumulated LW↓ anomaly time series. (c) Depth to permafrost table (DPT), and (d) change in soil heat content (ΔSHC) for three different initial permafrost states; $\overline{T_{soil}(\mathrm{PT}, \mathrm{y}=1)}$ = −0.3°C, −1.5°C, and −5.8°C from left to right.

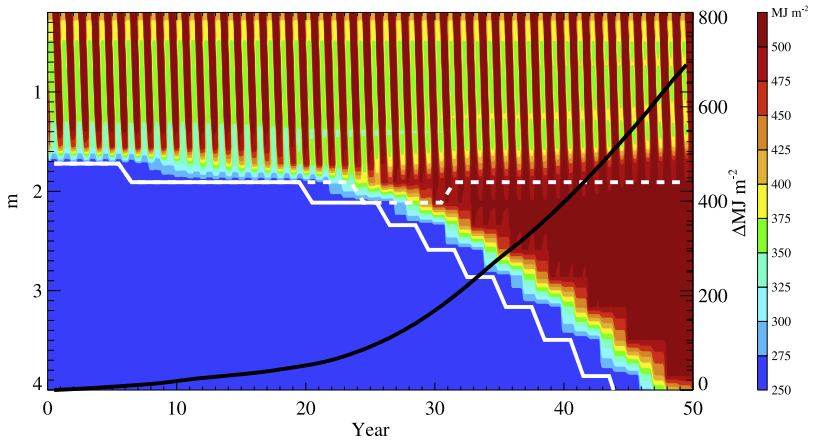

Figure 4. Time series of depth of warming (white solid line) and cooling (white dashed line) fronts from LINEAR experiment for warm permafrost case. Contours indicate SHC. Change in SHC is shown as black line.

[2006] find a dramatic increase in permafrost degradation in association with a 2° to 5°C warming in central Alaska over the period 1989–1998. *Isaksen et al.* [2007] argue that large T_{air} anomalies, such as those recently observed on Svalbard, are likely to hasten permafrost degradation.

[17] An abrupt change in Arctic climate is likely to have additional impacts beyond those on permafrost. Ecosystems, particularly sensitive ones such as those found in the Arctic, may be vulnerable to rapid change. Arctic ecosystems are already displaying a propensity for sudden change with recent observations indicating increased shrubbiness, longer growing seasons, advancing treelines, shifting migratory bird ranges, and declining caribou herd health [*Hinzman et al.*, 2005]. Positive feedbacks in the Arctic system could amplify these changes [*McGuire et al.*, 2006]. Enhanced permafrost degradation may itself alter tundra ecosystems and biogeochemical cycling through the formation of thermokarst and the redistribution of surface water [*Jorgenson et al.*, 2006]. Lastly, rapid near-term permafrost degradation would have implications for infrastructure planning.

5. Summary

[18] We find that rapid sea ice loss forces a strong acceleration of Arctic land warming in CCSM3 (3.5-fold increase, peaking in autumn) which can trigger rapid degradation of currently warm permafrost and may increase the vulnerability of colder permafrost for subsequent degradation under continued warming. Our results also suggest that talik formation may be a harbinger of rapid subsequent terrestrial change. This sea ice loss – land warming relationship may be immediately relevant given the record low sea ice extent in 2007.

[19] **Acknowledgments.** This research was supported by the Office of Science (BER), U. S. DOE, Cooperative Agreement DE-FC02-97ER62402 and NSF grants ARC-0229769, ARC-0531040, and ARC-C0629300. NCAR is supported by the National Science Foundation. We thank two anonymous reviewers for their constructive comments.

References

Beltrami, H., J. E. Smerdon, H. N. Pollack, and S. P. Huang (2002), Continental heat gain in the global climate system, *Geophys. Res. Lett.*, *29*(8), 1167, doi:10.1029/2001GL014310.

Collins, W. D., et al. (2006a), The Community Climate System Model Version 3 (CCSM3), *J. Clim.*, *19*, 2122–2143, doi:10.1175/JCLI3761.1.

Collins, W. D., P. J. Rasch, B. A. Boville, J. J. Hack, J. R. McCaa, D. L. Williamson, B. P. Briegleb, C. M. Bitz, S.-J. Lin, and M. Zhang (2006b), The formulation and atmospheric simulation of the Community Atmosphere Model Version 3 (CAM3), *J. Clim.*, *19*, 2144–2161, doi:10.1175/JCLI3760.1.

Hinzman, L. D., et al. (2005), Evidence and implications of recent climate change in northern Alaska and other arctic regions, *Clim. Change*, *72*, 251–298, doi:10.1007/s10584-005-5352-2.

Holland, M. M., C. M. Bitz, E. C. Hunke, W. H. Lipscomb, and J. L. Schramm (2006a), Influence of the sea ice thickness distribution on polar climate in CCSM3, *J. Clim.*, *19*, 2398–2414, doi:10.1175/JCLI3751.1.

Holland, M. M., C. M. Bitz, and B. Tremblay (2006b), Future abrupt reductions in the summer Arctic sea ice, *Geophys. Res. Lett.*, *33*, L23503, doi:10.1029/2006GL028024.

Intergovernmental Panel on Climate Change (IPCC) (2007), *Climate Change 2007: The Physical Science Basis. Contribution of Working Group I to the Fourth Assessment Report of the Intergovernmental Panel on Climate Change*, edited by S. Solomon et al., Cambridge Univ. Press, Cambridge, U. K.

Isaksen, K., R. E. Benestad, C. Harris, and J. L. Sollid (2007), Recent extreme near-surface permafrost temperatures on Svalbard in relation to future climate scenarios, *Geophys. Res. Lett.*, *34*, L17502, doi:10.1029/2007GL031002.

Jones, P. D., D. E. Parker, T. J. Osborn, and K. R. Briffa (2006), Global and hemispheric temperature anomalies: Land and marine instrumental records, in *Trends: A Compendium of Data on Global Change*, http://cdiac.esd.ornl.gov/trends/temp/jonescru/jones.html, *Carbon Dioxide Inf. Anal. Center, Oak Ridge Natl. Lab., U.S. Dep. of Energy, Oak Ridge, Tenn.*

Jorgenson, M. T., Y. L. Shur, and E. R. Pullman (2006), Abrupt increase in permafrost degradation in Arctic Alaska, *Geophys. Res. Lett.*, *25*, L02503, doi:10.1029/2005GL024960.

Lawrence, D. M., and A. G. Slater (2007), Incorporating organic soil into a global climate model, *Clim. Dyn.*, *30*, 145–160, doi:10.1007/s00382-007-0278-1.

Lawrence, D. M., A. G. Slater, V. E. Romanovsky, and D. J. Nicolsky (2008), Sensitivity of a model projection of near-surface permafrost degradation to soil column depth and inclusion of soil organic matter, *J. Geophys. Res.*, *113*, F02011, doi:10.1029/2007JF000781.

McGuire, A. D., F. S. Chapin, J. E. Walsh, and C. Wirth (2006), Integrated regional changes in Arctic climate feedbacks: Implications for the Global Climate System, *Annu. Rev. Environ. Resour.*, *31*, 61–91, doi:10.1146/annurev.energy.31.020105.100253.

Meehl, G. A., W. M. Washington, B. D. Santer, W. D. Collins, J. M. Arblaster, A. Hu, D. M. Lawrence, H. Teng, L. E. Buja, and W. G. Strand (2006), Climate change in the 20th and 21st centuries and climate change commitment in the CCSM3, *J. Clim.*, *19*, 2597–2616, doi:10.1175/JCLI3746.1.

Nicolsky, D. J., V. E. Romanovsky, V. A. Alexeev, and D. M. Lawrence (2007), Improved modeling of permafrost dynamics in a GCM land-surface scheme, *Geophys. Res. Lett.*, *34*, L08501, doi:10.1029/2007GL029525.

Oleson, K. W., et al. (2008), Improvements to the Community Land Model and their impact on the hydrological cycle, *J. Geophys. Res.*, *113*, G01021, doi:10.1029/2007JG000563.

Qian, T., A. Dai, K. E. Trenberth, and K. W. Oleson (2006), Simulation of global land surface conditions from 194 8 to 200 2: Part I: Forcing data and evaluations, *J. Hydrometeorol.*, *7*, 953–975, doi:10.1175/JHM540.1.

Serreze, M. C., and J. A. Francis (2006), The Arctic amplification debate, *Clim. Change*, *76*, 241–264, doi:10.1007/s10584-005-9017-y.

Stroeve, J., and W. Meier (1999, updated 2006), Sea Ice Trends and Climatologies From SMMR and SSM/I, http://nsidc.org/data/smmr_ssmi_ancillary/area_extent.html, Natl. Snow and Ice Data Cent., Boulder, Colo.

Stroeve, J., M. Serreze, S. Drobot, S. Gearhead, M. Holland, J. Maslanik, W. Meier, and T. Scambos (2008), Arctic sea ice plummets in 2007, *Eos Trans. AGU*, *89*, 13–14, doi:10.1029/2008EO020001.

C. Deser, M. M. Holland, D. M. Lawrence, and R. A. Tomas, NCAR/CGD, P.O. Box 3000, Boulder, CO 80307, USA. (dlawren@ucar.edu)

A. G. Slater, Cooperative Institute for Research in Environmental Sciences, University of Colorado, Campus Box 449, Boulder, CO 80309–0449, USA.